metals

MDPI

Article

Influences of Laser Spot Welding on Magnetic Property of a Sintered NdFeB Magnet

Baohua Chang [1,*], Dong Du [1], Chenhui Yi [1], Bin Xing [1] and Yihong Li [2]

[1] State Key Laboratory of Tribology, Department of Mechanical Engineering, Tsinghua University, Beijing 100084, China; dudong@tsinghua.edu.cn (D.D.); yich06@163.com (C.Y.); xingb13@126.com (B.X.)
[2] Taiyuan Tuolituo Technology Co. Ltd., Taiyuan 030032, China; liyihongtongli@aliyun.com
* Correspondence: bhchang@tsinghua.edu.cn; Tel.: +86-10-6278-1182

Academic Editor: Giuseppe Casalino
Received: 11 May 2016; Accepted: 22 August 2016; Published: 26 August 2016

Abstract: Laser welding has been considered as a promising method to join sintered NdFeB permanent magnets thanks to its high precision and productivity. However, the influences of laser welding on the magnetic property of NdFeB are still not clear. In the present paper, the effects of laser power on the remanence (Br) were experimentally investigated in laser spot welding of a NdFeB magnet (N48H). Results show that the Br decreased with the increase of laser power. For the same welding parameters, the Br of magnets, that were magnetized before welding, were much lower than that of magnets that were magnetized after welding. The decrease in Br of magnets after laser welding resulted from the changes in microstructures and, in turn, the deterioration of magnetic properties in the nugget and the heat affected zone (HAZ) in a laser weld. It is recommended that the dimensions of nuggets and HAZ in laser welds of a NdFeB permanent magnet should be as small as possible, and the magnets should be welded before being magnetized in order to achieve a better magnetic performance in practical engineering applications.

Keywords: laser welding; NdFeB magnet; magnetic property; process parameters

1. Introduction

NdFeB rare earth permanent magnets have been widely used in many industrial fields, such as aeronautics, astronautics, automotive, appliance, computers, and communications, thanks to their excellent magnetic property [1–3]. Sintered NdFeB permanent magnets are brittle and with poor mechanical properties. Therefore, in practical applications, the magnets are often joined with other materials using adhesive bonding or mechanical joining methods, which, however, have lower productivity and are hard to be applied on miniature structures [4–6].

Due to the high quality, high efficiency, and unrelenting repeatability, lasers have been widely applied in many materials processing processes, such as welding [7–13], cutting [14–16], additive manufacturing [17–20], and so on, and they have been used to process many types of materials, including metals, ceramics, glass, and polymers. Owing to the high power density, the laser generally results in welds with high precision and a small heat affected zone (HAZ) and, therefore, is considered as a good candidate to join the tiny sintered NdFeB components. However, studies carried out so far on the laser welding of sintered NdFeB magnet are still very limited. Microstructures and mechanical behavior have been studied for laser welds of NdFeB magnets [21] and laser welds of dissimilar materials of a NdFeB magnet and mild steel [22]. Nevertheless, it is still not clear how the laser welding will affect the magnetic property and how the optimal magnetic performance can be obtained. As we know, the magnetic property and performance are critical for the NdFeB permanent magnetic functional material in engineering applications, which makes it stringent to understand the change in the magnetic response of NdFeB when subject to laser welding processing.

In this paper, the influences of laser power on the magnetic property in terms of remanence are studied experimentally in micro-laser spot welding of an NdFeB permanent magnet, and the causes of the influences have been analyzed.

2. Materials and Methods

Sintered powder NdFeB permanent magnets N48H, without coating on surfaces, were used in this study. The compositions of the material are listed in Table 1. The Nd-Fe-B alloy particles with diameters of 3–5 microns were pressed and then sintered at 1060 °C for 2 h under vacuum conditions, followed by two tempering processes, which are 900 °C for 2 h, and 500 °C for 2 h, respectively. The microstructures of the magnet are shown in Figure 1, from which it can be seen that the main magnetic phase ($Nd_2Fe_{14}B$) of the magnet is gray and distributed non-uniformly, the white parts are the Nd-rich phase existing along grain boundaries or at intersections of grain boundaries of the main phase, and there exist certain amounts of voids which formed in the powder metallurgy process. The magnets were cut into specimens with dimensions of 7.5 × 3.5 × 0.7 mm.

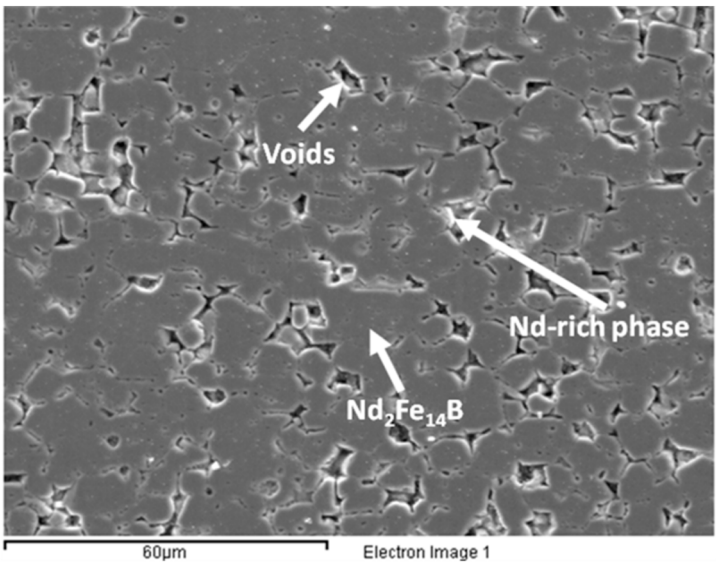

Figure 1. Microstructure of a NdFeB permanent magnet.

Table 1. Chemical compositions of the sintered NdFeB permanent magnet N48H (wt %).

Elements	Nd	Fe	B	Pr	Dy	Co	Cu	Nb
Contents	20.63	66.75	1.00	6.88	2.99	1.50	0.15	0.10

An IPG Photonics YLS-2000 (2 kW) (IPG Photonics, Oxford, MS, USA) type continuous waveform (cw) fiber laser was used in the welding trials, which had a wavelength of 1064 nm, and maximum power output of 2 kW. A schematic of welding setup is shown in Figure 2. Laser spot welds were made on the specimens at different laser powers, with a defocusing distance of +1 mm. The surfaces of the magnets were ground prior to welding to remove oxide layer, and 99.99% high-purity argon was used to protect the spot welds from oxidation, with a flow rate of Ar of 10 L/min. After welding, the spot welds were mounted, ground, polished, and then chemically etched with 4% nitric acid alcohol. Optical microscopy (Olympus, Tokyo, Japan) was employed to observe the shapes and dimensions of weld spots, and scanning electronic microscopy (SEM) (Hitachi, Tokyo, Japan) was used to analyze the microstructures of spot welds.

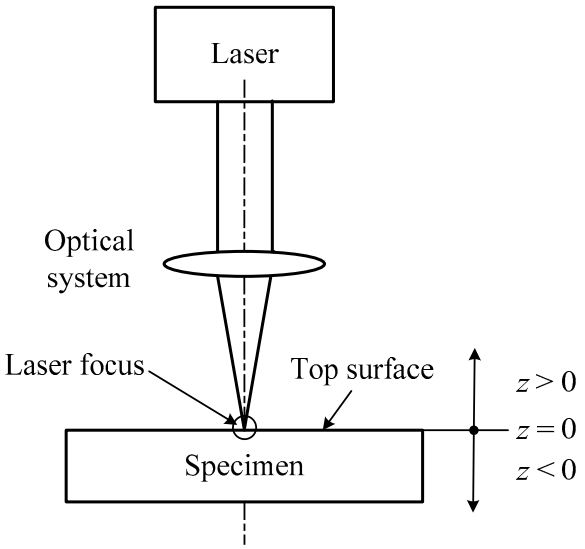

Figure 2. Schematic setup of laser spot welding of sintered NdFeB.

The remanence, Br, is one of the main parameters used to characterize the magnetic property of materials. In this study, the magnetic fluxes generated in coils by magnets were measured using a TA102E-1 type maxwellmeter (MKY, Beijing, China), in order to quantify the variation in remanence after laser welding. Two sequences were used in the present study. In the first sequence, the magnets were firstly magnetized, then spot welded by laser, and finally the remanences were measured; in the second sequence, the magnets were firstly welded by laser, then magnetized, and finally the measurements of remanences were carried out.

3. Results

3.1. Effects of Laser Power on Weld Dimensions

During laser welding of the sintered NdFeB, the materials with temperatures higher than the melting point (1180 °C) of the main phase $Nd_2Fe_{14}B$ will completely melted and form weld pools, and upon cooling, will finally form a nugget in a weld. The materials with temperatures ranging between 655 °C (melting point of Nd-rich phase) and 1180 °C will only partially melted, i.e., the Nd-rich phase will melt, while the main phase will not. This part of the material forms the heat affected zones (HAZ) in a weld spot. For materials with temperatures lower than 655 °C, melting will not take place, and the base metal of magnet is not affected as far as the microstructure is concerned. The constitution of a laser spot weld of the sintered NdFeB is shown in Figure 3a, in which two geometric parameters, i.e., surface diameter D_s and penetration depth P_n, are defined to characterize the dimensions of the spot weld. From Figure 3a, two different regions can be noticed in the nugget and, based on previous study [21], it has been found that they represent the columnar grain zone along fusion line (the interface between nugget and HAZ), and the equiaxed grain zone in the middle part of the nugget, respectively. The dashed lines in Figure 3a represent the boundaries between the nugget, HAZ, and base metal. Figure 3b more clearly shows the three distinct regions in a laser weld. The boundary between the base metal and the HAZ can be identified by whether the Nd-rich phase is melted or not.

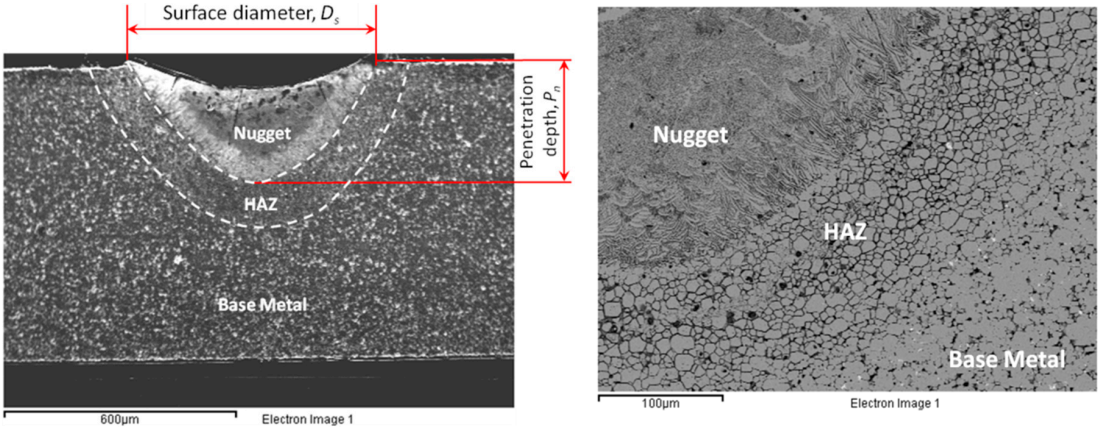

Figure 3. Constitution of a laser spot weld of the sintered NdFeB: (**a**) Definition of characteristic dimensions; (**b**) Three typical regions in a laser weld.

Dimensions of the weld spots produced with different laser powers ranging from 80 W to 180 W are given in Figure 4, from which it can be seen that the penetration depths increase monotonically for increased laser power, and a full penetration (0.7 mm) spot weld is obtained with a laser power of 180 W. The surface diameters of weld spots increase when increase the laser power from 80 W to 160 W, while a slight decrease in surface diameter can be noted with a further increase in the laser power from 160 W to 180 W. This can be attributed to the transition from partial penetration to full penetration of welds, which promotes the heat transfer in depth direction while reducing it in the radial direction. This phenomenon has also been reported in continuous laser welding trials with aluminum alloys [23].

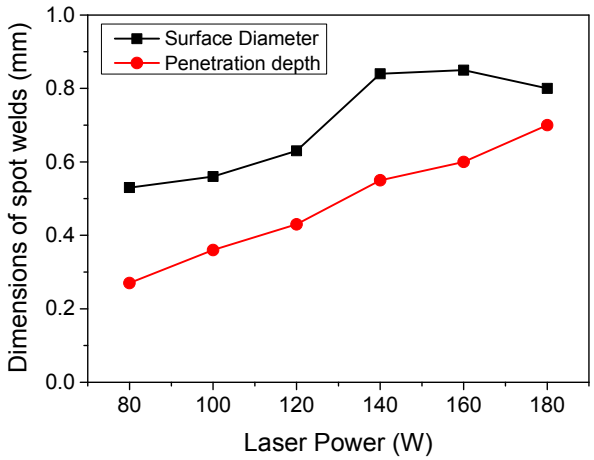

Figure 4. Dimensions of spot welds fabricated with different laser powers (weld time: 0.05 s, defocusing distance: +1 mm).

3.2. Effects of Laser Power on Magnetic Property

Figure 5 presents the effect of laser power on the magnetic flux. It can be seen that for the magnets welded before being magnetized, the magnetic flux decreased slightly for increased laser power. The minimum magnetic flux of 142.3 mWb was obtained at a laser power of 180 W, which was 6.5% lower than that of the magnets not welded, which was 152.2 mWb. For the magnets welded after being magnetized, the magnetic flux also decreased with the increasing of laser power, and the decrease was much more significant than the magnets welded before being magnetized. It can be seen that a 45.0% reduction in magnetic flux was caused by laser welding with a laser power of 180 W, resulting in a magnetic flux of 83.7 mWb.

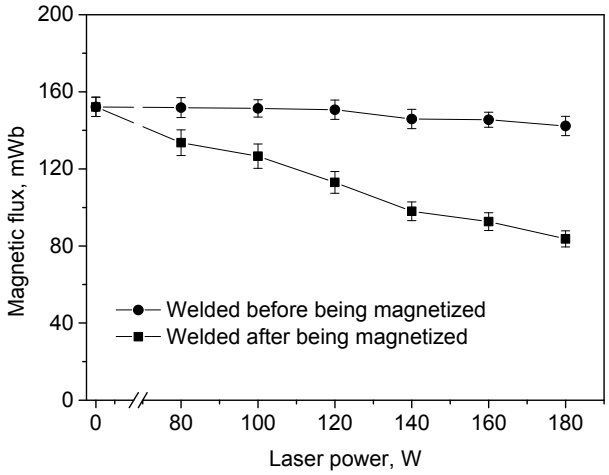

Figure 5. Effect of laser power on magnetic flux.

4. Discussion

4.1. Characteristics of Microstructures of a Laser Spot Weld

The cross-sections of laser spot welds of the magnet were observed by SEM. Similar microstructure features were found for welds made with different laser powers, despite the different dimensions of nuggets and heat affected zones, as indicated in the preceding section. As a representative, the microstructure of a partial penetrated spot weld (shown in Figure 6a) is presented here. Figure 6b demonstrates the details of section A of the nugget shown in Figure 6a. It can be seen from Figure 6b that the nugget of a NdFeB spot weld is composed mainly by ultra-fine grains of isotropic $Nd_2Fe_{14}B$, with disordered orientations. The different grain orientations of different regions are the result of epitaxial growth of columnar grains from fusion line, in addition to the growth of equiaxed grains in all directions during solidification [21]. According to the Stoner-Wohlfarth model [3], the remanence (Br) of isotropic NdFeB permanent magnets with a single easy magnetization axis is one half of the saturation magnetization (Bs) of the magnet. In contrast, the Br of anisotropic NdFeB permanent magnets with single easy magnetization axis is approximately equal to Bs. Obviously, the change in microstructure of nugget region from anisotropic to isotropic due to the melting and solidification during laser welding will deteriorate the magnetic property of the magnet.

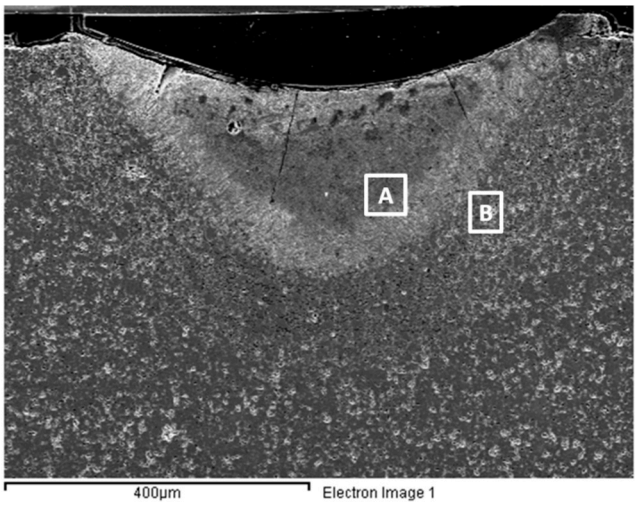

(**a**)

Figure 6. *Cont.*

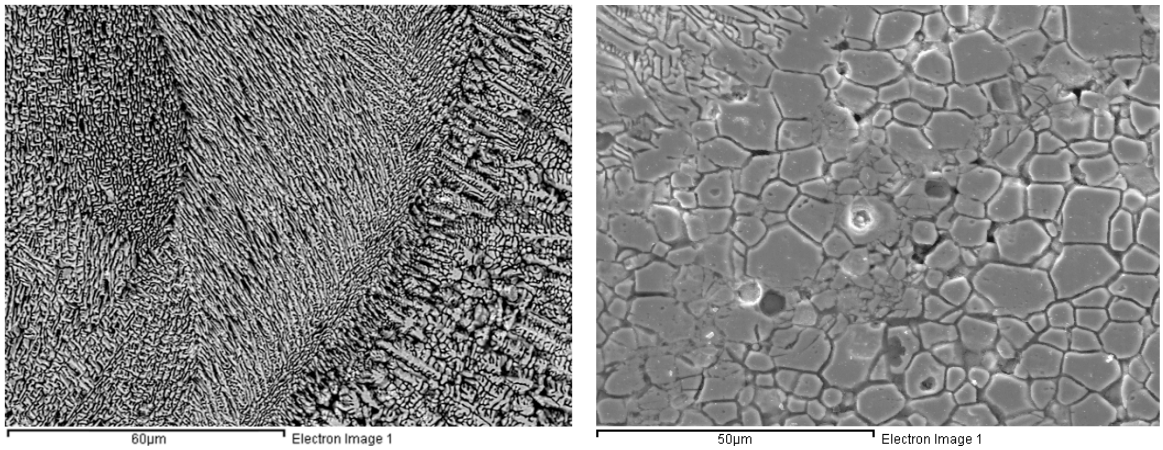

(**b**) (**c**)

Figure 6. The cross-section of laser spot weld (**a**); and the microstructures of nugget (**b**) and HAZ (**c**) in a laser spot weld.

Figure 6c presents the details of the heat affected zone (section B in Figure 6a). It can be seen that the melting of Nd-rich phase at grain boundaries will result in micro gaps and consequently weaken the bonding between grains of main phase $Nd_2Fe_{14}B$. Some main phase grains may be broken into small pieces, which may rotate when the melted Nd-rich phase flows locally. In this way, the orientation of the easy magnetization axes of these grains will deviate from their original orientation, which may result in the decrease in the degree of orientation and, in turn, the deterioration of the magnetic property.

4.2. Characteristics of Thermal Demagnetization of NdFeB

According to the experimental studies on the magnetic domains and magnetic property of NdFeB [24,25], the thermal demagnetization behavior of a NdFeB permanent magnet can be described with the curve shown in Figure 7. The magnetic property is basically unchanged for temperatures lower than the maximum working temperature (about 120 °C); for temperatures of 120 °C < T < 240 °C, the magnetic property decreases slightly; for T > 240 °C, the magnetic property decreases dramatically, and when the temperature is greater than about 300 °C (Curie temperature of NdFeB), the magnetic property disappears completely.

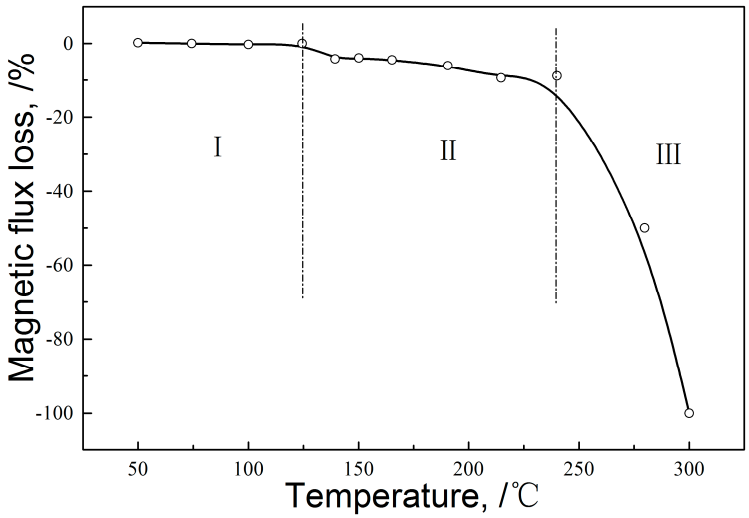

Figure 7. Thermal demagnetization curve of NdFeB permanent magnets [24,25].

4.3. Divisions of Regions in a Laser Spot Weld of NdFeB

Based on the discussion above, a spot weld of the NdFeB magnet can be divided into five regions, as shown in Figure 8.

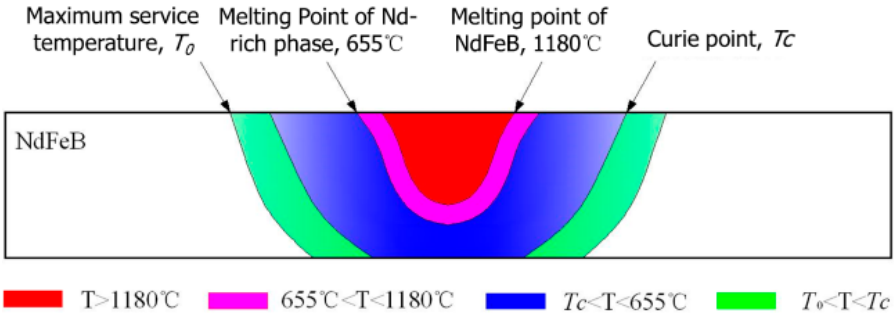

Figure 8. Schematic of temperature distribution and different regions in a spot weld of NdFeB permanent magnet.

The first region is nugget region that experiences temperatures above the melting point of magnet (1180 °C), which has lower magnetic property than the base metal due to its isotropic ultra-fine solidification structures, and the magnetic property of this region is not recoverable by magnetization.

The second region is heat affected zone, which experiences temperatures from the melting point of Nd-rich phase (655 °C) to that of base metal (1180 °C). It has lower magnetic property than base metal because of the melting of Nd-rich phase and in turn the weakened bonding between main phase grains. Similar to the nugget region, the magnetic property of this region is also not recoverable by magnetization.

The third region experiences temperatures ranging from the Curie point of the magnet (about 300 °C) to the melting point of the Nd-rich phase (655 °C) during the welding process. The magnetic property of this region will be reduced to zero if the magnet is magnetized, and can be fully recovered by re-magnetization after welding because the microstructure is not affected by welding.

The fourth region has temperatures ranging from the maximum working temperature (about 120 °C) to the Curie point of the magnet (about 300 °C) in laser welding. The magnetic property of this region will be partially reduced if the magnet is magnetized, and can be fully recovered by re-magnetization after welding.

The last region is the part with temperatures lower than 120 °C during welding, both microstructure and magnetic property of this region are not influenced by welding.

For magnets laser welded after being magnetized, the magnetic property of regions with temperatures higher than the maximum working temperature 120 °C (regions 1–4 as discussed above) is affected, which lead to a notable decrease in magnetic flux as shown in Figure 5. In contrast, for those magnets laser welded before being magnetized, although the magnetic properties of regions 1–4 may also be affected by welding, the magnetic properties of region 3 and 4 can be fully recovered. As a result, the deterioration of magnetic property is much less than those welded after magnetization. In order to obtain a better magnetic performance, it is recommended that the NdFeB permanent magnets should be welded before being magnetization in practical engineering applications, while the dimensions of nuggets and HAZ should be as small as possible.

5. Conclusions

(1) The magnetic property (in terms of Br) of NdFeB decreases with the increase of laser power. For the same welding parameters, the magnetic property of magnets that were magnetized before laser welding is much lower than that of magnets that were magnetized after laser welding.

(2) The decrease in the magnetic property of magnets after laser welding results from the changes in microstructures and, in turn, the deterioration of magnetic properties in the nugget and the heat affected zone (HAZ) in a laser weld.

(3) In order to obtain better magnetic performance, it is recommended that the NdFeB permanent magnets should be welded before being magnetized in practical engineering applications, while the dimensions of nuggets and HAZ should be as small as possible.

Acknowledgments: This research was supported by a Marie Curie International Incoming Fellowship with the 7th European Community Framework Programme (Grant No. 919487), whose financial support is gratefully appreciated.

Author Contributions: Baohua Chang and Dong Du conceived and designed the experiments; Chenhui Yi and Bin Xing performed the experiments and analyzed the data; Yihong Li contributed NdFeB materials used in the study; Baohua Chang wrote the paper.

Conflicts of Interest: The authors declare no conflict of interest.

References

1. Croat, J.J.; Herbst, J.F.; Lee, R.W.; Pinkerton, F.E. Pr-Fe and Nd-Fe-based materials: A new class of high-performance permanent magnets. *J. Appl. Phys.* **1984**, *55*, 2078–2082. [CrossRef]
2. Shield, J.E.; Zhou, J.; Aich, S.; Ravindran, V.K.; Skomski, R.; Sellmyer, D.J. Magnetic reversal in three-dimensional exchange-spring permanent magnets. *J. Appl. Phys.* **2006**, *99*, 08B508. [CrossRef]
3. Zhou, S.Z.; Dong, Q.F. *Super Permanent Magnet: Rare Earth Iron Series Permanent Magnet*, 2nd ed.; Metallurgical Industry Press: Beijing, China, 2004.
4. Je, S.S.; Rivas, F.; Diaz, R.E.; Kwon, J.; Kim, J.; Bakkaloglu, B.; Kiaei, S.; Chae, J. A compact and low-cost MEMS loudspeaker for digital hearing aids. *IEEE Trans. Biomed. Circuits Syst.* **2009**, *3*, 348–358. [CrossRef] [PubMed]
5. Kim, H.J.; Kim, D.H.; Koh, C.S.; Shin, P.S. Application of polar anisotropic NdFeB ring-type permanent magnet to brushless DC motor. *IEEE Trans. Magn.* **2007**, *43*, 2522–2524. [CrossRef]
6. Mosca, E.; Marchetti, A.; Lampugnani, U. Laser welding of PM Materials. *Powder Metall. Int.* **1983**, *15*, 115–118.
7. Chang, B.H.; Allen, C.; Blackburn, J.; Hilton, P.; Du, D. Fluid Flow Characteristics and Porosity Behavior in Full Penetration Laser Welding of a Titanium Alloy. *Metall. Mater. Trans. B* **2015**, *46*, 906–918. [CrossRef]
8. Casalino, G.; Campanelli, S.L.; Ludovico, A.D. Laser-arc hybrid welding of wrought to selective laser molten stainless steel. *Int. J. Adv. Manuf. Technol.* **2013**, *68*, 209–216. [CrossRef]
9. Casalino, G.; Mortello, M. Modeling and experimental analysis of fiber laser offset welding of Al-Ti butt joints. *Int. J. Adv. Manuf. Technol.* **2016**, *83*, 89–98. [CrossRef]
10. Kuryntsev, S.V.; Gilmutdinov, A.K. The effect of laser beam wobbling mode in welding process for structural steels. *Int. J. Adv. Manuf. Technol.* **2015**, *81*, 1683–1691. [CrossRef]
11. Casalino, G.; Mortello, M.; Leo, P.; Benyounis, K.Y.; Olabi, A.G. Study on arc and laser powers in the hybrid welding of AA5754 Al-alloy. *Mater. Des.* **2014**, *61*, 191–198. [CrossRef]
12. Kuryntsev, S.V.; Gilmutdinov, A.K. Heat treatment of welded joints of steel 0.3C-1Cr-1Si produced by high-power fiber lasers. *Opt. Laser Technol.* **2015**, *74*, 125–131. [CrossRef]
13. Wu, S.J.; Gao, H.M.; Zhang, Z.Y. A preliminary test of a novel molten metal filler welding process. *Int. J. Adv. Manuf. Technol.* **2015**, *80*, 647–655. [CrossRef]
14. Hilton, P.A.; Lloyd, D.; Tyrer, J.R. Use of a diffractive optic for high power laser cutting. *J. Laser Appl.* **2016**, *28*, 012014. [CrossRef]
15. Kaakkunen, J.J.J.; Laakso, P.; Kujanpaa, V. Adaptive multibeam laser cutting of thin steel sheets with fiber laser using spatial light modulator. *J. Laser Appl.* **2014**, *26*, 032008. [CrossRef]
16. Hilton, P.; Khan, A.; Walters, C. The laser alternative. *Nucl. Eng. Int.* **2010**, *55*, 18–20.
17. Xing, B.; Chang, B.H.; Yang, S.; Du, D. A study on the cracking behaviour in laser metal deposition of IC10 directionally solidified nickel-based superalloy. *Mater. Res. Innov.* **2015**, *19*, 281–285. [CrossRef]
18. Sexton, L.; Lavin, S.; Byrne, G.; Kennedy, A. Laser cladding of aerospace materials. *J. Mater. Proc. Technol.* **2002**, *122*, 63–68. [CrossRef]

19. Casalino, G.; Campanelli, S.L.; Contuzzi, N.; Ludovico, A.D. Experimental investigation and statistical optimisation of the selective laser melting process of a maraging steel. *Opt. Laser Technol.* **2015**, *65*, 151–158. [CrossRef]
20. Campanelli, S.L.; Angelastro, A.; Signorile, C.G.; Casalino, G. Investigation on direct laser powder deposition of 18 Ni (300) marage steel using mathematical model and experimental characterization. *Int. J. Adv. Manuf. Technol.* **2016**. [CrossRef]
21. Chang, B.H.; Yi, C.H.; Du, D.; Zhang, H.; Li, Y.H. Characteristics of microstructures in laser spot welds of a sintered NdFeB permanent magnet for different welding modes. *J. Tsinghua Univ. Sci. Technol.* **2014**, *54*, 1138–1142.
22. Chang, B.H.; Bai, S.J.; Du, D.; Zhang, H.; Zhou, Y. Studies on the micro-laser spot welding of an NdFeB permanent magnet with a low carbon steel. *J. Mater. Proc. Technol.* **2010**, *210*, 885–891. [CrossRef]
23. Chang, B.H.; Blackburn, J.; Allen, C.; Hilton, P. Studies on the spatter behaviour when welding AA5083 with a Yb-fibre laser. *Int. J. Adv. Manuf. Technol.* **2016**, *84*, 1769–1776. [CrossRef]
24. Luo, Y.; Zhang, N.; Su, X.J. Thermal analysis and domain observation of Nd-Fe-B magnet. *Acta Metall. Sin.* **1987**, *23*, 136–140.
25. Zhang, N.; Luo, Y. Thermal analysis of Nd-Fe-B magnet. *J. Iron Steel Res.* **1986**, *6*, 91–98.